

Sensitivity study of a sapphire detector using Coherent Elastic Neutrino-Nucleus Scattering process

S. P. Behera^{1,2*}

¹*Nuclear Physics Division, Bhabha Atomic Research Centre,
Mumbai - 400085, India and*

²*Homi Bhabha National Institute, Anushakti Nagar, Mumbai - 400094, India*

The Indian Coherent Neutrino-nucleus Scattering Experiment(ICNSE) has been proposed at Bhabha Atomic Research Centre in India to measure the coherent elastic neutrino-nucleus scattering process using electron antineutrinos produced from reactors. Phenomenological studies are performed to find out the sensitivity of sapphire detector for various fundamental physics parameters at an exposure of one year. Reactors of different core compositions, sizes, and thermal powers have been considered as sources of electron antineutrinos. The potential of the ICNSE to measure the weak mixing angle at a low energy regime has been extracted. Furthermore, the detector's capability has been investigated for examining the electromagnetic properties of neutrinos, including their magnetic moment. Additionally, an exploration has been conducted on the detector's sensitivity in restricting new interactions between neutrinos and electrons or nuclei, thereby constraining the parameter space related to light mediators. It is found that the ICNSE detector can put a stronger constraints on the scalar and vector mediators masses.

I. INTRODUCTION

The concept of coherent elastic neutrino-nucleus scattering (CE ν NS) was initially introduced by Freedman [1] within the framework of the standard model (SM) of particle physics. The CE ν NS process involves low-energy neutrinos scattering off the entire atomic nucleus via neutral-current interactions within the SM of weak interactions. For low momentum transfer, CE ν NS cross section is approximately proportional to number of neutrons present in the target nuclei. In the CE ν NS process, the nuclei that are scattered carry energy on the order of keV. Measurement of such low energy recoil nuclei is extremely difficult. In contrast, this interaction channel provides a significantly higher interaction rate per target atom, ranging from 3 to 4 orders of magnitude, when compared to other detection methods like inverse beta decay and neutrino electron scattering [2]. As a result, it enables a significantly smaller target size than the traditional neutrino detectors. Conversely, an experiment with a large target mass can obtain high neutrino statistics, allowing for precise measurements of various neutrino parameters.

The COHERENT group has recently conducted the first measurements on the CE ν NS process [3] with accelerator neutrinos at the Spallation Neutron Source. They observed the process at a 6.7σ confidence level using a low-background CsI[Na] scintillator. In the following years, the group reported a second measurement in an LAr detector [4], and another data set from the CsI measurement has been released [5]. The measured cross section is consistent with the standard model prediction. They also have the first-ever detection of the CE ν NS process on germanium nuclei with a significance of 3.9σ [6]. The measurement of the CE ν NS cross-section provides a pathway to explore a variety of physics phenomena across different research fields including particle physics, nuclear physics, astrophysics, and cosmology. Studying the CE ν NS process can shed light on fundamental aspects of

physics beyond the SM, such as the non-standard interactions [7], the neutrino magnetic moment [8], the weak mixing angle [7, 9], and the nuclear neutron density distributions. Furthermore, the possible existence of sterile neutrinos could be confirmed or disproved by observing neutrinos through the flavor-blind (CE ν NS) process. This process also allows for detailed investigations into the interiors of dense objects and stellar evolution [10, 11]. The CE ν NS process not only offers to explore the Beyond Standard Model (BSM) physics but also can be applied for monitoring nuclear reactors. In India, an experimental setup the Indian Coherent Neutrino-nucleus Scattering Experiment(ICNSE), has been proposed to measure the CE ν NS cross section using electron antineutrinos produced from the reactor and address various fundamental physics aspects.

The current study examines the detection capabilities of the ICNSE detector for measuring the weak mixing angle, neutrino magnetic moment, and masses of various mediators. The weak mixing angle has been measured at higher energy in GeV scale [12], while the measurement at low energy requires improved accuracy of this parameter [13, 14]. The cross section for CE ν NS depends on the weak charge, aiding in the study of the weak mixing angle at extremely low momentum transfer. With the established fact that neutrinos possess non-zero mass from the neutrino oscillation experiment, they are expected in the extension of the SM to exhibit electromagnetic properties such as neutrino magnetic moment and neutrino charge radius. The nuclear recoil energy spectrum can be distorted due to neutrino interaction with nuclei in the presence of a magnetic moment. Further neutrinos coupling to protons and neutrons may be potentially influenced due to the non-standard interaction of neutrinos. Then it introduces additional new parameters that can provide insight into the relative magnitude of these interactions compared to the neutral-current weak interaction as described in the the SM [15]. These couplings can be expressed as a function of the mediator mass and the momentum transfer. In case of a momentum transfer greater than the mediator mass, the couplings exhibit transfer momentum dependence, which leads to the possibility of new physics phenomena, such as the in-

* shiba@barc.gov.in

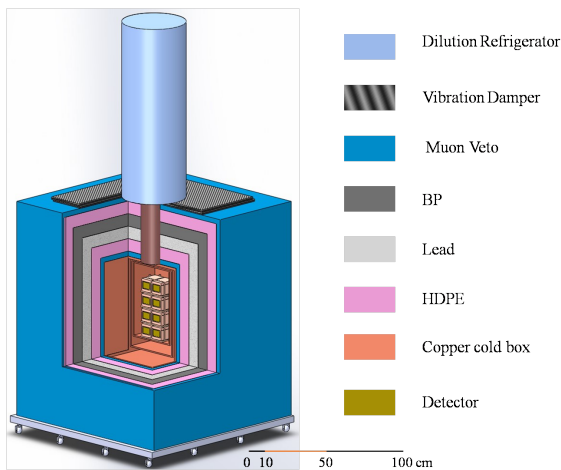


FIG. 1. Schematic representation of the ICNSE experimental setup for $CE\nu NS$ process measurement. BP: borated polyethylene, thickness: 10 cm; HDPE: high-density polyethylene, thickness: 10 cm. The figure has been taken from Ref. [16].

roduction of a new gauge symmetry featuring an additional scalar or vector mediator. A scalar or vector particle can participate in $CE\nu NS$ process and potentially alter the nuclear recoil spectrum in a unique way. The characteristic distortion of the spectrum shape for light scalars with masses around the neutrino energy allows us to reconstruct the scalar mass. The COHERENT group has put a limit on its mass and coupling with SM particles [3].

The article is organized as follows. In the following section, a detailed description of the proposed ICNSE setup is presented. The production mechanism of neutrinos inside the reactor is elaborated in Sec. III. The $CE\nu NS$ process and the principle of measurement are discussed in Sec. IV. The procedure for estimating the expected number of events in the detector is described in Sec. V. The sensitivity of the proposed experiment and statistical method on χ^2 estimation considered in this study are discussed in Sec. VI. The sensitivity of the detector to various physics parameters at an exposure of one year is elaborated in Sec. VII. In Sec. VIII, observations obtained from this study are summarized, and the implication of this work are discussed.

II. PROPOSED ICNSE DETECTOR SETUP FOR $CE\nu NS$ PROCESS MEASUREMENT

As mentioned earlier that, experiments based on $CE\nu NS$ process require detectors with very low threshold that are essential for the measurement of very low nuclear recoil energies (\sim few keV). Semiconductor detectors based on germanium or silicon are good candidates to achieve the very low threshold required. However, the energy thresholds of such detectors are $\mathcal{O}(\text{keV})$ which is also very high to observe $CE\nu NS$ process using reactor antineutrinos. Recoil energies can be measured using cryogenic detectors, which can achieve excellent energy resolutions along with low thresholds. Cryo-

genic detectors can be made from a lot of different materials, such as semiconductors like germanium or insulators like calcium tungstate and sapphire (Al_2O_3). However, sapphire is a very good candidate to observe $CE\nu NS$ due to the lower atomic mass of Al and O , making it sensitive to lower nuclear recoil energies. Sapphire has good phononic properties and it has already been shown that low energy thresholds $\mathcal{O}(0.1\text{keV})$ are possible with these crystals. A baseline recoil energy resolution of 18 eV that corresponds to a recoil energy threshold of 54 eV has been achieved using a scale of 100 g newly developed sapphire detector [17]. According to a sensitivity study carried out in Ref. [18], the $CE\nu NS$ process can be measured at a 5σ level using cryogenic detectors with recoil energy thresholds of 20 eV. Thus, for the present work, only sapphire has been used as a target material. The conceptual design of the detector setup has been considered from Ref. [16] which is shown in Fig 1.

Additionally, the assessment of low nuclear recoil energy is influenced by background noise originating from both the reactor core and environmental factors. These background sources encompass gamma rays and neutrons emitted by the reactor, as well as muons and muon-induced neutrons resulting from cosmic rays and surrounding gamma radiation from natural radioactivity. The energy-dependent backgrounds attributed to neutrons and gamma rays are evaluated in Ref. [19]. Also, several rare event search experiments observe sharply rising backgrounds at sub-keV energies close to their respective thresholds that are larger than expected from known backgrounds [20]. Therefore, it is essential to suppress natural and reactor related backgrounds comprising mostly of gamma-rays, neutrons, and muons. This is achieved by using a multilayer structure shielding materials as shown in Fig. 1. The outermost layer of this shielding is a 4 cm thick plastic scintillator (PS) for vetoing external radiation. This is followed by 10 cm thick layers of high-density polyethylene (HDPE) and borated polyethylene (BP) sheets containing 15% boron for thermalizing fast neutrons and subsequently attenuating them. This is followed by 10 cm layer of lead shielding to attenuate gamma radiation. An additional layer of 10 cm thick HDPE followed by a 4 cm thick PS are placed inside the lead layers to thermalize and tag any fast neutrons produced in the lead layer via (γ, n) reactions or muon-induced neutrons. The detectors are housed in an oxygen-free high thermal conductivity (OFHC) copper cold box placed at the center of this shielding. The copper box also shields the detector from charged radiation. The thickness of lead and BP sheets was decided considering an earlier study [21] carried out for the Indian Scintillator Matrix for Reactor Anti-Neutrino, an inverse beta decay reaction based reactor antineutrino experiment. To maintain the required cryogenic temperatures (about 15 mK for α -phase of W [22]) for the detector operation, a dilution refrigerator is placed on top of the shielding. A cold finger will establish the thermal link for cooling the cold box from the dilution refrigerator. It is also important to take the precaution of ensuring proper thermal link for stable operation while damping out vibrations from reaching the detector setup. The signal extraction method from the sapphire detector is described below.

TABLE I. Various types of reactors used as $\bar{\nu}_e$ sources

Reactors name	Thermal power(MW _{th})	Fuel type	Core sizes, R: radius, H: Height
U-Apsara	3.0	U ₃ Si ₂ -Al (17% enriched ²³⁵ U)	R = 0.32 m, H = 0.64 m
Dhruva	100.0	Natural uranium (0.7% ²³⁵ U)	R = 1.5 m, H = 3.03 m
PFBR	1250.0	MOX(PuO ₂ -UO ₂)	R = 0.95 m, H = 1.0 m
VVER	3000.0	UO ₂ (3.92 % enriched ²³⁵ U)	R = 1.58 m, H = 3.53 m

In the CE ν NS process process, the recoiling nucleus induces athermal excitation in the detector crystal, with approximately 92% of the energy being converted into generating athermal phonons and remaining energy goes for producing scintillating photon signals. Consequently, the recoil energy of nuclei can be determined by monitoring the signals stemming from phonons. Additionally, the phonon signals are not contingent on the nature of the interaction $i.e$ signals due to either electron recoil or nuclear recoil as the detector is a calorimetric device [18, 23]. From the ICNSE experimental setup, phonons will be identified through a dual-stage procedure employing quasiparticle-trap-assisted electrothermal-feedback transition-edge-sensors made up of Al fins coupled to tungsten Transition Edge Sensors(W-TES), fabricated on the surface of the detector. The measurement process involves the collection of phonons by the aluminum fins, leading to the disruption of cooper pairs and the generation of quasi-particles. Subsequently, these quasi-particles disperse throughout the aluminum fins until they are captured in the overlap region, where they enter into tungsten, inducing a rise in temperature. By maintaining tungsten within its superconducting transition range, this temperature fluctuation results in a significant alteration in resistance, which is quantified by applying a current through the W-TES under voltage biased mode [17].

III. PRODUCTION OF ELECTRON ANTI-NEUTRINOS FROM THE REACTOR

Man-made nuclear reactor are intense sources of pure $\bar{\nu}_e$ s. On average, 10^{20} $\bar{\nu}_e$ s are produced from a 1 GW_{th} thermal power reactor. In a reactor, $\bar{\nu}_e$ s are produced mainly by two processes. One of them is the beta decay of neutron-rich fission fragments of mainly four isotopes, such as ²³⁵U, ²³⁸U, ²³⁹Pu, and ²⁴¹Pu. Each isotope has a different fission rate which leads to different $\bar{\nu}_e$ s yield and spectrum. $\bar{\nu}_e$ s have a maximum energy of about 10 MeV, which is produced from the beta decay of fission fragments. Another important one is from the neutron capture process by the ²³⁸U that leads to the production of two $\bar{\nu}_e$ s having energy <1.3 MeV [24]. This process accounts for approximately 16% of the overall $\bar{\nu}_e$ flux. These low energy neutrinos are usually neglected, as most of the experiments detect $\bar{\nu}_e$ through the inverse beta decay process. It can be noted here that the relative contribution of each isotope to the total $\bar{\nu}_e$ s flux depends on the fuel composition of the reactors and their burning cycle. There is also a small variation in flux that occurs due to fuel burn-up. The present study has been carried out considering various types of reactors with

different core sizes, compositions, and thermal power. Details on reactor thermal power, compositions, and core sizes are given in Table I. At present, it is planned to put the detector at 4 m from the reactor core in the Apsara-U research reactor facility at Bhabha Atomic Research Centre (BARC), India [25]. The main advantage of the Apsara-U reactor is that it has a movable and compact core. The utilization of a mobile core offers the benefit of mitigating systematic uncertainties associated with the reactor and the detector through the implementation of position-specific measurements. In the future, the same detector setup can be placed at other reactor facilities such as Dhruva, BARC [26], proto-type fast breeder reactor (PFBR), IGCAR, Kalpakkam [27], and VVER, Kudankulam in India [28].

IV. MEASUREMENT OF THE COHERENT NEUTRINO NUCLEUS SCATTERING PROCESS

The measurement of the CE ν NS process provides a probe to study the BSM physics. The differential CE ν NS scattering cross-section is given by

$$\frac{d\sigma}{dT}(E_\nu, T) = \frac{G_F^2}{8\pi} Q_W^2 \times M \left(2 - \frac{TM}{E_\nu^2} \right) |f(q)|^2 \quad (1)$$

and $Q_W = Z(4\sin^2\theta_W - 1) + N$. In Eq. 1, M, N , and Z are the mass, number of neutrons, and number of protons in the nucleus, respectively. Further, E_ν is the incident neutrino energy, T is nuclear recoil energy, ($T_{\max}(E_\nu) = 2E_\nu^2/(M + 2E_\nu)$), G_F is the Fermi coupling constant, θ_W is the weak mixing angle, and $f(q)$ is the nuclear form factor for a momentum transfer of q . It can be noted that Eq. 1 is applicable for all types of neutrinos and antineutrinos. For low energy neutrinos ($E_\nu < 50$ MeV), the momentum transfer is very small such that $q^2 R^2 < 1$, where R is the radius of the nucleus, which leads $f(q) \sim 1$. At small momentum transfers, the scattering amplitude from individual nucleons is in phase and adds coherently, which leads to the increase of the cross-section. The weak mixing angle $\sin^2\theta_W$ has been measured to be $0.23867 \pm 0.00016 \sim 1/4$ [13]. Then, the contribution from the proton is suppressed, that leads the cross-section proportional to N^2 . Therefore, it is possible to detect neutrinos via the CE ν NS process with kg-size detectors due to high event rates. Further, it can be observed that the recoil energy is inversely proportional to the mass number of the target. At a given E_ν , although the cross section can be enhanced by choosing a heavier nucleus, the measurable recoil energy is lowered at the same time. Therefore, it is required to consider

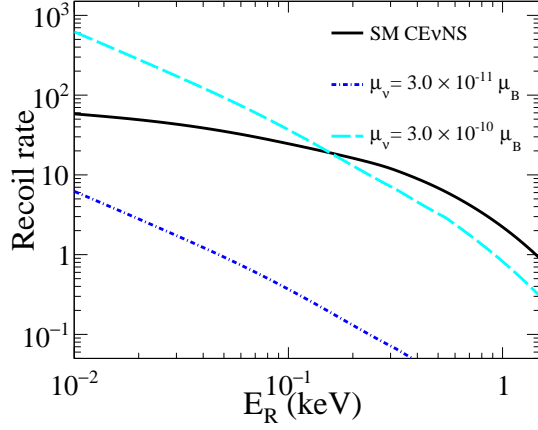


FIG. 2. Recoil event rate per day as a function of nuclear energy at different values of neutrino magnetic moment for the sapphire detector of mass 10 kg is placed at a 4 m from the Apsara-U reactor core.

the target materials with intermediate atomic numbers that is a good compromise between the experimental observable that corresponds is the detection rate and detection possibility. It has been previously noted that measurement of low nuclear recoil energy of few keV presents a significant challenge, necessitating the minimization of low energy backgrounds in relevant measurements and the enhancement of accuracy in the CE ν NS experimental approach. It is observed from Eq. 1 that the cross section depends on weak mixing angle which provides a complimentary measurement at low momentum transfer by measuring the signal due to low energy of recoil nuclei. Further, the measurement of neutrino magnetic moment and other physics aspects can be addressed using the CE ν NS process, which is discussed in the following subsections.

A. The CE ν NS process due to the magnetic moment of neutrino

In minimal extensions of the SM with three right-handed neutrinos, the magnetic moment μ_ν is predicted to be non-zero with values ranging from less than 10^{-14} to $10^{-19} \mu_B$, where μ_B represents the Bohr magneton. The neutrino magnetic moment is a result of loop-level radiative correction [29]. In contrast, theories extending beyond the minimal extended SM, the neutrino magnetic moment could be on the order of $10^{-(10-12)} \mu_B$ for Majorana neutrinos, while for Dirac neutrinos, it can not exceed $10^{-14} \mu_B$. Hence, the observation of neutrino magnetic moment can provide insight into the nature of neutrinos. The Super-Kamiokande Collaboration has put an upper limit of $3.6 \times 10^{-10} \mu_B$ at a 90% confidence level (C.L.) using solar neutrino spectra above 5-MeV. It has been further improved to a limit of $1.1 \times 10^{-10} \mu_B$ (90% C.L.) considering additional information from other solar neutrino and KamLAND experiments [30]. The BOREXINO group has placed a constraint on the magnetic moment of neutrinos using solar neutrinos, establishing an upper limit of the effective nuclear magnetic moment as $\mu_\nu < 2.8 \times 10^{-11}$ at a 90%

C.L. [31]. The best magnetic moment limit from the reactor antineutrinos based GEMMA experiment is $2.9 \times 10^{-11} \mu_B$ (90% C.L.) [32]. Various groups have also placed constraints on the neutrino magnetic moment using neutrinos from different sources [33–35].

The neutrino-nucleus scattering cross section modifies in the presence of a neutrino magnetic moment. In the simplified model framework, the scattering cross section is given by

$$\frac{d\sigma^{mag}}{dT}(E_\nu, T) = \frac{\pi\alpha^2\mu_\nu^2 Z^2}{m_e^2} \left[\frac{1}{T} - \frac{1}{E_\nu} + \frac{T}{4E_\nu^2} \right] f(q)^2 \quad (2)$$

In the above equation, α is the fine structure constant, μ_ν is the magnetic moment of the neutrino, m_e is the mass of the electron. The recoil rate due to neutrino-nucleon magnetic scattering depends upon $1/T$ whereas its strength is controlled by the size of the effective neutrino magnetic moment in units of Bohr magnetons μ_B . Experimentally, a signature of a nonzero neutrino magnetic moment can be observed via distortion of the recoil spectrum of coherently scattered nuclei. The recoil event rate as a function of nuclear recoil energy is shown in Fig. 2 at various values of neutrino magnetic moment for 10 kg sapphire detector placed at a 4 m distance from the Apsara-U reactor core for an exposure of 1 year. It can be observed that at lower recoil energy the recoil rate due to the SM CE ν NS process is much flatter than the recoil rate from the electromagnetic interaction of neutrinos due to their magnetic moment. The later rate increases with increasing the magnetic moment. Further, it is observed that at the lower recoil energy, the more considerable increase in the neutrino magnetic moment effect with respect to the SM CE ν NS process. So the detector with a lower threshold can differentiate the neutrino magnetic moment effect against the standard CE ν NS process.

B. The CE ν NS process due to the exchange of massive mediators

A new scalar particle ϕ can participate in the CE ν NS process, which mediates an interaction between neutrinos and quarks. This results the modification of nuclear recoil energy spectrum, both for a light scalar as well as a heavy one. The interaction Lagrangian is given by

$$\mathcal{L}_\phi = \phi [g_\nu \bar{\nu}_R \nu_L + g_\nu^* \bar{\nu}_L \nu_R + g_\ell \bar{\ell} \ell + g_u \bar{u} u + g_d \bar{d} d] \quad (3)$$

where $\nu_{L,R}$, are left- and right-handed neutrinos, $\ell = e, \mu$, and τ are charged leptons, and u, d are up- and down-type quarks. It is noted here that the exchange of this new scalar mediator does not interfere with Standard Model Z -exchange. Then the modified SM CE ν NS cross section due to ϕ exchange is expressed as [36, 37]

$$\frac{d\sigma_\phi}{dT} = \frac{G_F^2}{4\pi} Q_\phi^2 \left(\frac{2MT}{E_\nu^2} \right) m_N F^2(q). \quad (4)$$

In Eq. 4 presented above, the scalar mediator's mass is denoted as m_ϕ , the nuclear charge due to ϕ exchange is represented by Q_ϕ , and the momentum transfer is calculated

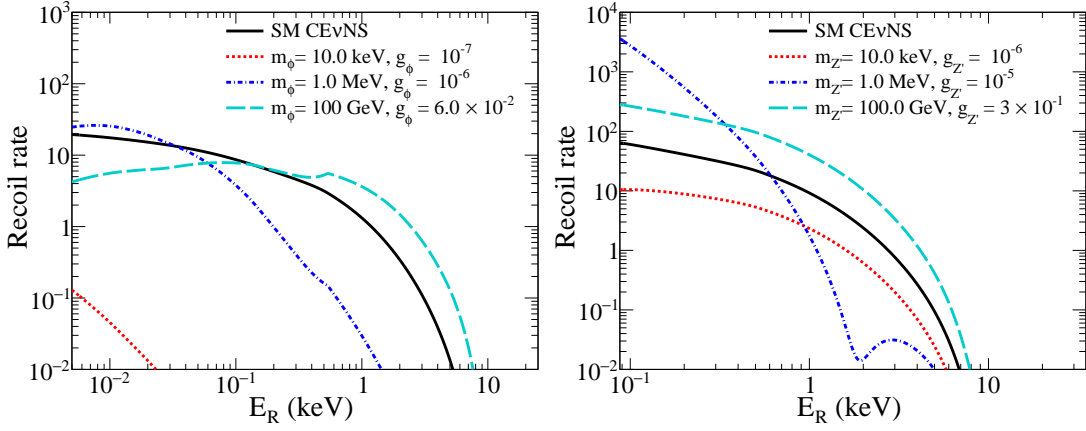


FIG. 3. Recoil event rate as a function of nuclear energy due to exchange the scalar(left panel) and the vector(right panel) mediators of different masses. The sapphire detector of mass 10 kg is placed at a 4 m from the Apsara-U reactor core.

TABLE II. Expected events rate in the sapphire detector for various reactor core to the detector distance and thermal power.

Reactors name	Distance from core (m)	Counts/day/kg
U-Apsara	4.0	0.42
Dhruva	10.0	3.25
PFBR	25.0	5.26
VVER	30.0	10.85

as $q = \sqrt{2MT}$. The determination of the nucleus's ‘scalar charge’ is approximated based on the quark couplings g_q and the quarks contributions to the nucleon. With the consideration for universal couplings to all quarks, an approximate formula is mentioned in Ref. [37] that is expressed as

$$Q_\phi = \frac{(15.1Z + 14N)g_\phi^2}{\sqrt{2}G_F(2MT + m_\phi^2)}, \quad (5)$$

where $g_\phi^2 = g_\nu g_q$, with g_ν is the neutrino coupling and g_q is the common coupling to quarks. Left panel of Fig. 3 illustrates the impact on the nuclear recoil rate caused by a scalar mediator, featuring various masses and couplings. Solid line shows the SM CEvNS rate and the contribution due to the exchange of scalars with different masses is shown in dashed(dashed-dotted) lines. It has been observed that for light mediators with masses less than or on the order of MeV, the interaction exhibits an effectively long-range behavior. This results in a recoil spectrum that rapidly decreases with momentum transfer and follows a relationship of q^{-4} ($\sim T^{-2}$). On the other hand, for heavier mediators, the spectrum becomes peaked, with the cross section scaling linearly with the recoil energy (T) at low energies. However, at high energies, the coherence is lost, leading to a cutoff in the spectrum. In a study by Farzan et al. [37], it is mentioned that if the mass of the new scalar is similar to the energy of the neutrinos, it should also be feasible to measure the mass of the mediator (m_ϕ). Similarly, the SM CEvNS cross section can be modified due to the presence of a new massive vector mediator that couples to SM neutrinos and quarks. In the present study we have considered a vector neutral current neutrino non-standard interaction with

quarks that exhibits a coherent nuclear enhancement due to contributions from Z and Z' exchange, leading to its typical dominance. Further, it is assumed that the exchange of this new vector mediator does not interfere with Standard Model Z -exchange. Due to the exchange of this vector mediator, Q_W is given in Eq. 1 is modified, which is given by [38]

$$Q_{SM+Z'} = Q_W - \frac{\sqrt{2}}{G_F} \frac{Q_{Z'}}{q^2 + m_{Z'}^2}, \quad (6)$$

where $Q_{Z'} = (2Z + N)g_u g_\nu + (2N + Z)g_d g_\nu$ which leads to a change in differential cross section. Right panel of Fig. 3 shows the effect on the nuclear recoil rate caused by a vector mediator of different masses and couplings. It is found that recoil rate increases at low energy due to the exchange of vector mediators with an increase in mass.

V. EVENT RATE IN A DETECTOR

A high CEvNS reaction cross section per unit detector mass is advantageous for detectors weighing in the kilogram range. The predicted events rate due to CEvNS can be calculated as

$$N_{\text{events}}^{\text{SM}} = \epsilon t \lambda_0 \frac{M_{\text{detector}}}{A} \int_{E_{\nu\text{min}}}^{E_{\nu\text{max}}} \lambda(E_\nu) dE_\nu \int_{T_{\text{min}}}^{T_{\text{max}}(E_\nu)} \left(\frac{d\sigma}{dT} \right) dT, \quad (7)$$

where M_{detector} is the mass of the detector, t is the time duration of data taking, λ_0 is the total neutrino flux, $\lambda(E_\nu)$ is the

TABLE III. List of systematic uncertainties considered in the analysis.

Uncertainties	Contribution(%)
Total neutrino flux, number of target atoms, and detector efficiency	5.0
Energy calibration	1.0
Nonlinear energy response	1.0

neutrino spectrum and ϵ is the efficiency of the detector. In the present study, the Hubber-Muller model [39, 40] parameterization has been considered for $\bar{\nu}_e$ s produce from beta decay of fission fragments of energy spectra above 2.0 MeV. The low energy part of the $\bar{\nu}_e$ s spectra is considered from Ref. [33, 41]. The antineutrinos produced from the slow neutron capture by the ^{238}U have energy < 2 MeV. We have considered the numerical data for this part of the spectrum from Ref. [33]. The minimum recoil energy of the nuclei in a specific experimental setup is determined by the detector threshold. We have chosen to analyze neutrinos with a maximum energy of approximately 10.0 MeV since there are fewer neutrinos above this energy. The number of events expected in the detector due to various reactor power as well as reactor core to the detector distance is listed in the Table. II. Event rate has been estimated assuming a detection energy threshold of 100 eV, 80% of the detection efficiency independent of nuclear recoil, 90% fiducial volume of the detector, 70% reactor duty cycle and, for an exposure of 1 day. Studies have been conducted using a target mass of 10 kg to extract the detector sensitivity for various parameters related to the CE ν NS process.

VI. SIMULATION METHOD AND EXTRACTION OF THE DETECTOR SENSITIVITY

The present study has been carried out to find the potential of the ICNSE detector on different physics parameters by using $\bar{\nu}_e$ s produced from various types of reactor facilities that is mentioned in Sec. III. The number of neutrinos produced from the reactor depends both on the thermal power as well as on fuel compositions. Electron antineutrinos flux produced from the reactor has different energy dependent for various isotopes. The parametrization for $\bar{\nu}_e$ flux assumed in the present analysis is mentioned in Ref. [16]. The number of events expected in the detector has been evaluated by knowing the energy dependent flux, cross-section, the detector efficiency, fiducial volume of the detector and the reactor duty cycle. Both the production point of neutrinos inside the reactor core and the interaction point in the detector are generated using a Monte-Carlo method. The sensitivity is evaluated by assuming that a given experiment searching for CE ν NS events will measure exactly the SM expectation; thus any deviation is understood as a signature of new physics. For this purpose, a statistical analysis between the predicted and expected event distribution obtained from simulation is carried out in order to quantify the sensitivity of the detector for a given exposure. The sensitivity of the detector to various parameters is extracted by estimating the χ^2 . The definition of the χ^2 is

taken from Ref. [42] and given as

$$\chi^2 = \frac{\xi^2}{\sigma_\xi^2} + \sum_{T \text{ bins}} \frac{[(1 + \xi)N_n^{th}(\xi) - N_n^{ex}]^2}{\sigma_{\text{stat},n}^2 + \sigma_{\text{sys},n}^2}, \quad (8)$$

where ξ denotes the pull parameter with uncertainty σ_ξ . In Eq. 8, N^{ex} , N^{th} are representing the number of events obtained from the simulations with the deviation from SM CE ν NS cross section (considered as measured) and with consideration of the SM CE ν NS cross section (considered as theoretically predicted) events, respectively. The procedure for estimating theoretically predicted events N_n^{th} with consideration of the reactor as well as the detector related parameters is mentioned in Ref.[16]. In both types of simulated events, the detector response such as resolution and efficiency are incorporated. The procedure for the detector response incorporation is mentioned in Ref. [16]. The statistical uncertainty $\sigma_{\text{stat},n}$ and the systematic uncertainty $\sigma_{\text{sys},n}$ of the event number in the n -th recoil energy bin are given by

$$\sigma_{\text{stat},n} = \sqrt{N_n^{th} + N_{\text{bkg},n}}, \quad \sigma_{\text{sys},n} = \sigma_f(N_n^{th} + N_{\text{bkg},n}) \quad (9)$$

Here $N_{\text{bkg},n}$ is the number of background events. We assume that $\sigma_{\text{sys},n}$ is proportional to the event number with a coefficient σ_f . The χ^2 is minimized with respect to pull variables ξ and it is estimated by considering different sources of systematic uncertainties as mentioned in Table III. It includes normalization uncertainty which arises due to reactor total neutrino flux, the number of target atoms, and the detector efficiency, uncertainty due to the nonlinear energy response of the detector and, uncertainty in the energy calibration. So an overall $\sigma_\xi = 5\%$ systematic uncertainty has been considered.

The measurement of low energy of recoil nuclei from the CE ν NS process faces a significant challenge due to the presences of both natural and reactor backgrounds such as gamma-rays and neutrons. The sensitivity of the detector is influenced not only by the various types of backgrounds but also by the energy-dependent configuration of these backgrounds. At low recoil energy, two distinct background shapes are observed: the $1/T$ shape and flat-shaped backgrounds, as referenced in Ref. [43]. The procedure for extracting the detector sensitivity due to the presence of different types of backgrounds is mentioned in [16]. Similarly the systematic uncertainty due to backgrounds is considered as $\sigma_f = 5\%$. A signal-to-background ratio of 1.0 and 2.0 has been taken into consideration to determine the sensitivity of the detector in the presence of background.

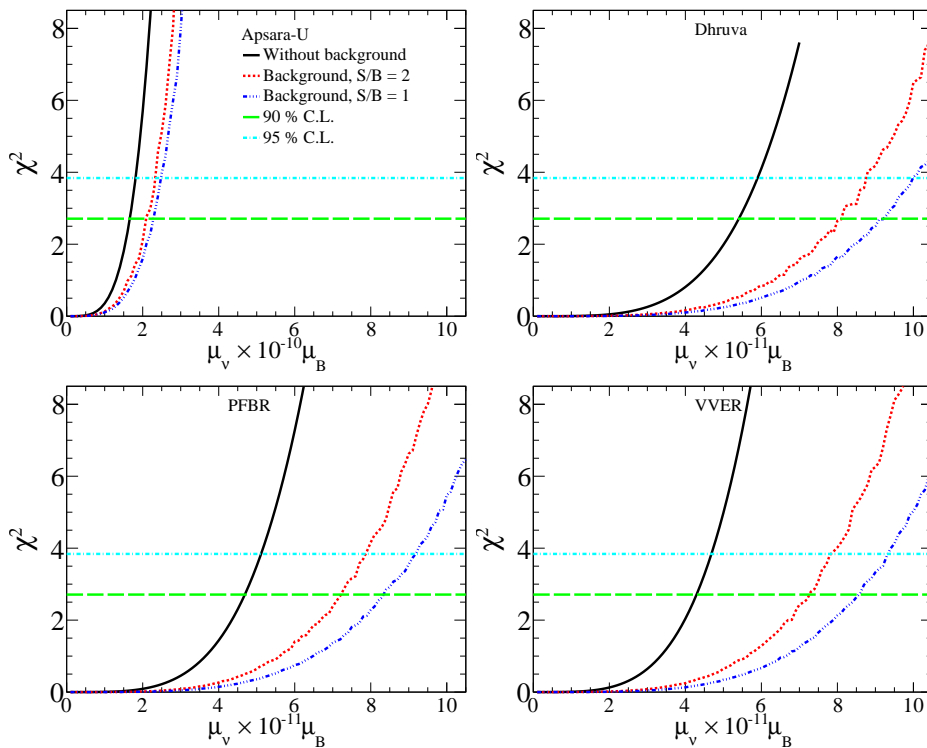


FIG. 4. Comparison of the ICNSE detector sensitivity to the neutrino magnetic moment considering with and without background.

VII. RESULTS AND DISCUSSIONS

The sensitivity of the detector to various physics parameters are computed considering the procedure mentioned above. Results based on this study are presented below.

A. Sensitive to the magnetic moment of neutrinos

The detector's sensitivity to the neutrino magnetic moment has been determined by analyzing the simulated events. The theoretically predicted events, which take into account the SM $\text{CE}\nu\text{NS}$ cross section, are compared with the simulated measured events estimated using the cross section affected by neutrino magnetic moments. It is found that the ICNSE detector has sensitivity to the interesting regimes of the neutrino magnetic moment. The detector sensitivity to the neutrino magnetic moment is shown in Fig. 4 taking into account the different reactor power and the distance of the reactor core to the detector as previously mentioned. In Fig. 4, solid and dotted(dashed-dotted) lines show the detector sensitivity considering without and with background, respectively. The results are compared with sensitivity at 90.0% and 95.0% C.L. It has been observed that the detector placed at the Apsara-U reactor can measure the neutrino magnetic moment for $\mu_B \geq 1.66 \times 10^{-10} \mu_B$ in the absence of background. The neutrino magnetic moment can be restricted even further below the level of $\mu_B \sim 5.4 \times 10^{-11}$, $\mu_B \sim 4.68 \times 10^{-11}$, and $\mu_B \sim 4.29 \times 10^{-11}$ at 90 % C.L. using the ICNSE de-

tor without having background, placing at a reactor with high power such as Dhruva, PFBR, and VVER facilities, respectively. The GEMMA experiment has put the strongest constraint on the neutrino magnetic moment using reactor antineutrinos, which is $< 2.9 \times 10^{-11} \mu_B$ (90% C.L.). Furthermore, the detector's sensitivity is extracted based on the backgrounds present at the experimental site. In the present study, a signal-to-background ratio(S/B) of 2.0 and 1.0 are considered. The detector sensitivity reduces with the inclusion of background, as demonstrated in Fig. 4. In the case of the detector placed at the Apsara-U reactor, it has been observed that the sensitivity reduced by about 25.9 % and 37.3% considering a signal-to-background ratio of 2.0 and 1.0, respectively, at 90.0 % C.L. The sensitivity of the detector reduces by about 50.0 % and 53.2% for S/B = 2.0 by placing it at the Dhruva and PFBR reactor facilities, respectively. Additionally, it has been bound that with increasing the systematic effect(σ_f) 10 % from 5%, the sensitivity of the detector has been reduced further by about 15.2% for S/B= 1.0 , considering the detector placed at 10m from the Dhruva reactor core.

B. Sensitive to the weak mixing angle

The weak mixing angle is one of the fundamental parameters of particle physics, which couples the electromagnetic and weak interactions. In the $\text{CE}\nu\text{NS}$ process, the cross-section is proportional to the weak charge Q_W^2 as mentioned in Eq. 1. Hence, the weak mixing angle can be extracted from the measured absolute cross section. In an experiment, it can

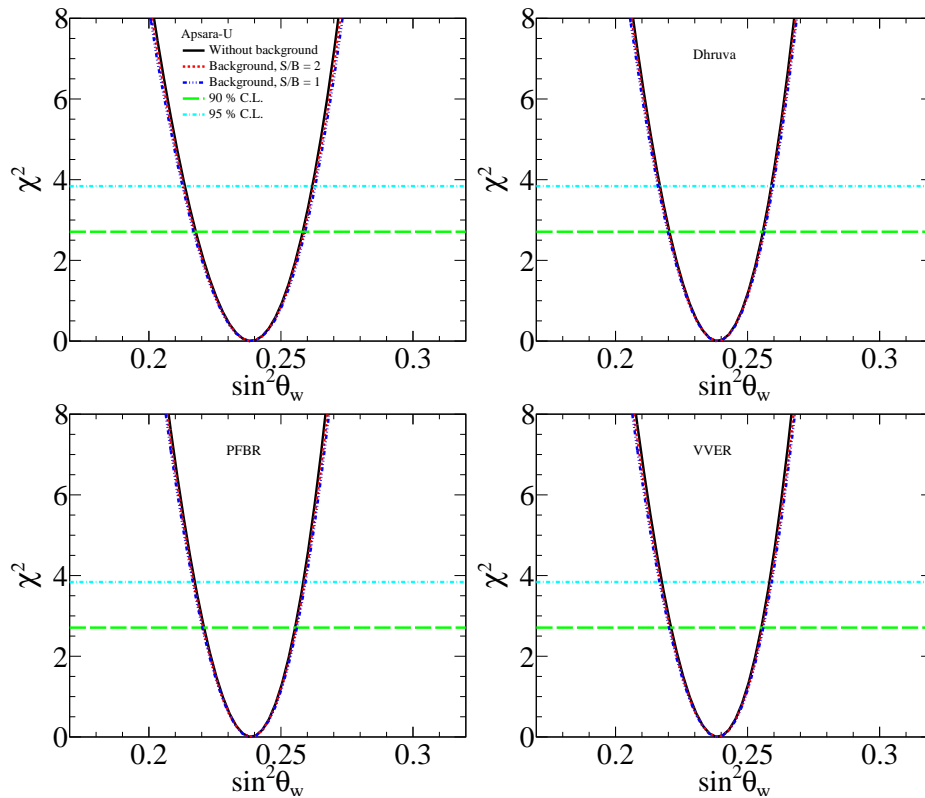


FIG. 5. Sensitivity of the detector to the weak mixing angle considering Apsara-U, Dhruva, PFBR, and VVER reactors as antineutrinos sources.

be measured by observing a deviation from the SM prediction of the weak mixing angle. It has been measured precisely by the Z-pole experiment at high energy. However, at low energy measurements are carried out with less precision. There are several measurements carried out at low energy, such as Qweak [44], and from the atomic parity violation experiments [45]. Further measurements by various group may improve the precision as mentioned in Refs. [46–48]. At low energy, the precision of weak mixing angle measurement may be improved by the $CE\nu NS$ process. The weak mixing angle sensitivity of the ICNSE detector has been extracted considering reactors of different thermal powers and at different reactor cores to the detector distance. The sensitivity has been extracted by estimating the chi square between the simulated events with consideration of SM weak mixing angle $\sin^2\theta_W = 0.2386$ and events generated by varying the weak mixing angle.

Figure 5 shows the possible sensitivity of the detector to weak mixing angle at 90% C.L. considering different reactors as neutrino sources. The uncertainty expected due to measurement has also been extracted. At 90% C.L., the width of the weak mixing angle $\delta\sin^2\theta_W$ is estimated as $(S_{W^{max}}^2 - S_{W^{min}}^2)/2$ and the corresponding uncertainty is $\delta\sin^2\theta_W/\sin^2\theta_W$, where $S_{W^{max}}$ and $S_{W^{min}}$ are the upper and lower limits values at 90% C.L., respectively. It has been observed that expected uncertainties on weak mixing angle measurements are about 8.59 %, 7.33 %, 7.33% and, 7.12% by placing the detector at Apsara-U, Dhruva, PFBR,

and VVER reactor facilities, respectively. A larger uncertainty arises due to the fact that the detector has a low Z target material. In order to improve the measurement sensitivity, it is necessary to have a highly intense neutrino source or a detector of larger mass, which reduce the statistical error. Further, it has been observed that the background has less impact on the detector sensitivity to the weak mixing angle. It has been bound that with increasing the systematic effect (σ_f) 10 % from 5%, the sensitivity of the detector to the weak mixing angle is further reduced to 8.59 % from 7.33 % for S/B= 1.0, considering the detector placed at 10m from the Dhruva reactor core.

C. Sensitive to the mass of mediators

The detector's sensitivity to the mediator mass has been extracted by estimating the chi-square between the number of events calculated using the SM $CE\nu NS$ cross section and with the deviation from SM $CE\nu NS$ cross section. Events are estimated with consideration of the SM $CE\nu NS$ cross section considered as theoretically predicted ones whereas events are estimated using the cross section influenced by to coupling of a new scalar or a vector mediator to fermions are considered as simulated measured ones. In $g_\phi - m_\phi$ plane, Fig. 6 shows the expected sensitivity of the ICNSE detector on the coupling of a new scalar mediator to fermion considering various types of reactor core to the detector distances as well as thermal power. It is assumed that scalar coupling to all SM

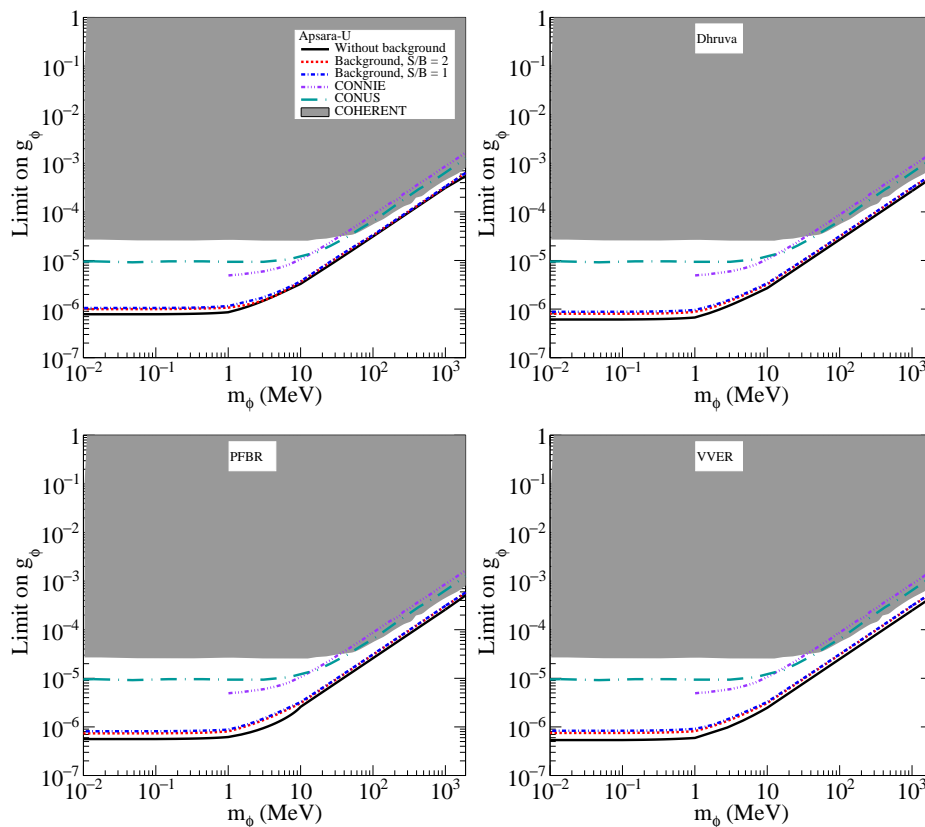


FIG. 6. The detector sensitivity to the scalar mediator at 90% C.L. The shaded portion is the excluded region from the COHERENT group.

fermions is universal. At lighter mass region, the detector's sensitivity is independent of mediator mass as the interaction cross section depends on only g_ϕ . For heavier scalar mass the interaction rate is proportional to g_ϕ/m_ϕ . At low mass (≤ 10.0 MeV) region, the sensitivity has been reduced due to the presence of background. It is found that detectors have similar sensitivity at higher scalar mass region. The ICNSE detectors can exclude most of the parameter space as excluded by the COHERENT group.

An expected potential sensitivity of the ICNSE detector to the mass of the vector mediator is shown in Fig. 7. It is found that the ICNSE detector can exclude most of the parameter space as well as the region excluded by the COHERENT group in $g_{Z'} - m_{Z'}$ plane. At low vector mediator mass region, a similar behavior has been observed as observed for scalar mediators. In the presence of background, the detector's sensitivity can deteriorates more at lower mass regions as compared to high mass regions. Results from the CONNIE [49] and the CONUS [2] experiments have been shown for the comparisons. At $S/B=1$ and mediators of mass less than 10 MeV, it has been bound that with increasing the systematic effect (σ_f) 10 % from 5%, the sensitivity of detector has been reduced about 12% and 5% due to the nonstandard interaction caused by scalar and vector mediators, respectively by considering the detector placed at a distance of 10 m from the Dhruva reactor core.

VIII. SUMMARY

The measurement of low energy recoil nuclei due to the $CE\nu NS$ process is very challenging. However, the recent measurement of the $CE\nu NS$ process by the COHERENT group opened a window to further explore physics beyond the standard model of particle physics. Currently, several studies are ongoing, and some studies are proposed to measure many important properties of neutrinos using different types of detectors, taking into account different sources of neutrinos. In this article, we have explored the physics potential of the sapphire detector in the context of the proposed $CE\nu NS$ scattering experiment in India. The study has been performed for a time horizon of 1 year employing $\bar{\nu}_e s$ produced from the research reactor, which can be further employed for the measurement at the power reactor. It is found that the detector has the potential to measure various BSM physics parameters such as neutrino magnetic moment and weak mixing angle using the $CE\nu NS$ process. The detector can limit most of the parameter space in $g_\phi - m_\phi$ as well as $g_{Z'} - m_{Z'}$ plane because of its lower energy thresholds. At low mass region of mediators, the background has more effect compared to higher mass regions. Further, the detector sensitivity can be improved by reducing background with a proper shielding.

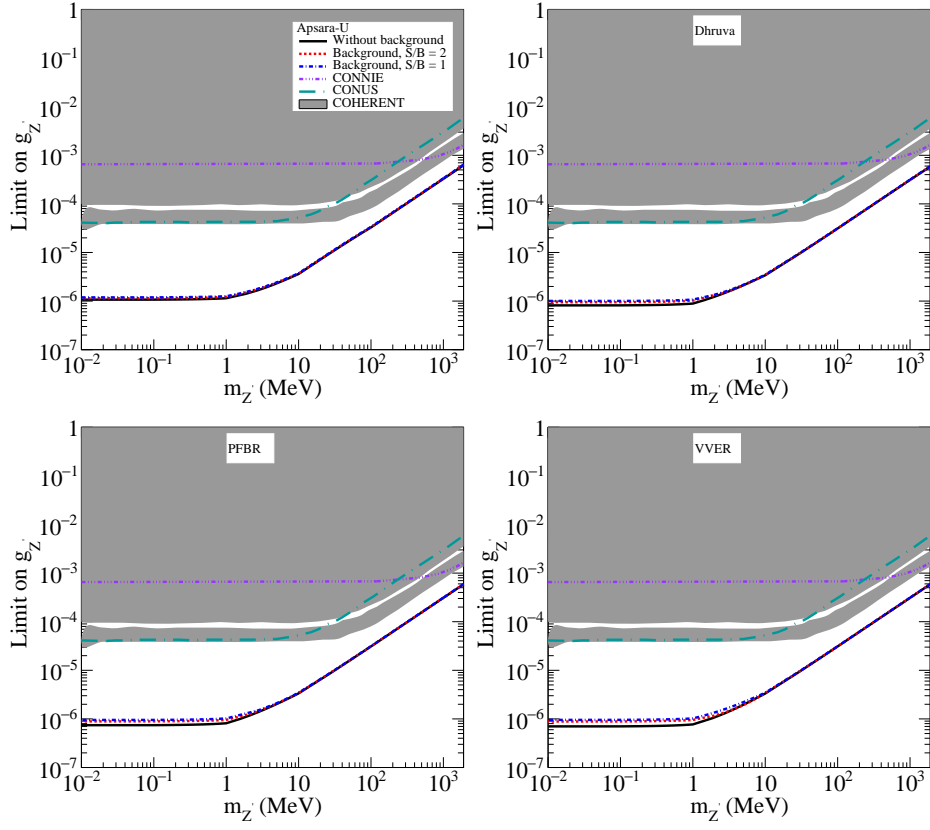


FIG. 7. The detector sensitivity to the vector mediator at 90% C.L. The shaded portion is the excluded region from the COHERENT group.

ACKNOWLEDGMENTS

The author thanks V. Jha, D. K. Mishra, Kirtikesh Kumar and, other group members of the ICNSE, BARC for useful suggestions and discussions. The author also thanks Dimitrios Papoulias and Luis Flores for giving critical comments on the manuscript.

-
- [1] D. Z. Freedman, *Phys. Rev. D* **9**, 1389 (1974).
[2] H. Bonet *et al.* (CONUS), *JHEP* **05**, 085 (2022), [arXiv:2110.02174 \[hep-ph\]](#).
[3] D. Akimov *et al.* (COHERENT), *Science* **357**, 1123 (2017), [arXiv:1708.01294 \[nucl-ex\]](#).
[4] D. Akimov *et al.* (COHERENT), *Phys. Rev. Lett.* **126**, 012002 (2021), [arXiv:2003.10630 \[nucl-ex\]](#).
[5] D. Akimov *et al.* (COHERENT), *Phys. Rev. Lett.* **129**, 081801 (2022), [arXiv:2110.07730 \[hep-ex\]](#).
[6] S. Adamski *et al.* (COHERENT), (2024), [arXiv:2406.13806 \[hep-ex\]](#).
[7] D. K. Papoulias and T. S. Kosmas, *Phys. Rev. D* **97**, 033003 (2018), [arXiv:1711.09773 \[hep-ph\]](#).
[8] T. S. Kosmas, O. G. Miranda, D. K. Papoulias, M. Tortola, and J. W. F. Valle, *Phys. Rev. D* **92**, 013011 (2015), [arXiv:1505.03202 \[hep-ph\]](#).
[9] B. C. Cañas, E. A. Garcés, O. G. Miranda, and A. Parada, *Phys. Lett. B* **776**, 451 (2018), [arXiv:1708.09518 \[hep-ph\]](#).
[10] M. Biassoni and C. Martinez, *Astropart. Phys.* **36**, 151 (2012), [arXiv:1110.3536 \[astro-ph.HE\]](#).
[11] V. Brdar, M. Lindner, and X.-J. Xu, *JCAP* **04**, 025 (2018), [arXiv:1802.02577 \[hep-ph\]](#).
[12] P. Vilain *et al.* (CHARM-II), *Phys. Lett. B* **335**, 246 (1994).
[13] J. Erler and M. J. Ramsey-Musolf, *Phys. Rev. D* **72**, 073003 (2005), [arXiv:hep-ph/0409169](#).
[14] B. C. Cañas, E. A. Garcés, O. G. Miranda, M. Tortola, and J. W. F. Valle, *Phys. Lett. B* **761**, 450 (2016), [arXiv:1608.02671 \[hep-ph\]](#).
[15] C. Giunti, *Phys. Rev. D* **101**, 035039 (2020), [arXiv:1909.00466 \[hep-ph\]](#).
[16] S. P. Behera, D. K. Mishra, P. K. Netrakanti, R. Sehgal, K. Kumar, R. Dey, and V. Jha, *Phys. Rev. D* **108**, 113002 (2023), [arXiv:2304.00912 \[hep-ph\]](#).
[17] S. Verma *et al.*, *Nucl. Instrum. Meth. A* **1046**, 167634 (2023), [arXiv:2203.15903 \[physics.ins-det\]](#).

- [18] R. Strauss *et al.*, *Eur. Phys. J. C* **77**, 506 (2017), [arXiv:1704.04320 \[physics.ins-det\]](#).
- [19] G. Agnolet *et al.* (MINER), *Nucl. Instrum. Meth. A* **853**, 53 (2017), [arXiv:1609.02066 \[physics.ins-det\]](#).
- [20] P. Adari *et al.*, *SciPost Phys. Proc.* **9**, 001 (2022), [arXiv:2202.05097 \[astro-ph.IM\]](#).
- [21] D. a. Mulmule, *Nucl. Instrum. Meth. A* **911**, 104 (2018), [arXiv:1806.04421 \[physics.ins-det\]](#).
- [22] A. Jastram, H. R. Harris, R. Mahapatra, J. Phillips, M. Platt, K. Prasad, J. Sander, and S. Upadhyayula, *Nucl. Instrum. Meth. A* **772**, 14 (2015), [Erratum: *Nucl.Instrum.Meth.A* 820, 172–172 (2016)], [arXiv:1408.0295 \[physics.ins-det\]](#).
- [23] M. Heikinheimo, S. Sassi, K. Nordlund, K. Tuominen, and N. Mirabolfathi, *Phys. Rev. D* **106**, 083009 (2022), [arXiv:2112.14495 \[hep-ph\]](#).
- [24] G. Fernandez Moroni, J. Estrada, E. E. Paolini, G. Canelo, J. Tiffenberg, and J. Molina, *Phys. Rev. D* **91**, 072001 (2015), [arXiv:1405.5761 \[physics.ins-det\]](#).
- [25] T. Singh, P. Pandey, T. Mazumdar, K. Singh, and V. Raina, *Annals of Nuclear Energy* **60**, 141 (2013).
- [26] S. Agarwal, C. Karhadkar, A. Zope, and K. Singh, *Nuclear Engineering and Design* **236**, 747 (2006), india's Reactors: Past, Present, Future.
- [27] S. Chetal, V. Balasubramanian, P. Chellapandi, P. Mohanakrishnan, P. Puthiyavinayagam, C. Pillai, S. Raghupathy, T. Shanmugham, and C. S. Pillai, *Nuclear Engineering and Design* **236**, 852 (2006), india's Reactors: Past, Present, Future.
- [28] S. Agrawal, A. Chauhan, and A. Mishra, *Nuclear Engineering and Design* **236**, 812 (2006), india's Reactors: Past, Present, Future.
- [29] S. Y. Lee, *Phys. Rev. D* **6**, 1701 (1972).
- [30] D. W. Liu *et al.* (Super-Kamiokande), *Phys. Rev. Lett.* **93**, 021802 (2004), [arXiv:hep-ex/0402015](#).
- [31] M. Agostini *et al.* (Borexino), *Phys. Rev. D* **96**, 091103 (2017), [arXiv:1707.09355 \[hep-ex\]](#).
- [32] A. G. Beda, V. B. Brudanin, V. G. Egorov, D. V. Medvedev, V. S. Pogosov, E. A. Shevchik, M. V. Shirchenko, A. S. Starostin, and I. V. Zhitnikov, *Phys. Part. Nucl. Lett.* **10**, 139 (2013).
- [33] H. T. Wong *et al.* (TEXONO), *Phys. Rev. D* **75**, 012001 (2007), [arXiv:hep-ex/0605006](#).
- [34] L. B. Auerbach *et al.* (LSND), *Phys. Rev. D* **63**, 112001 (2001), [arXiv:hep-ex/0101039](#).
- [35] R. C. Allen, H. H. Chen, P. J. Doe, R. Hausammann, W. P. Lee, X. Q. Lu, H. J. Mahler, M. E. Potter, K. C. Wang, T. J. Bowles, R. L. Burman, R. D. Carlini, D. R. F. Cochran, J. S. Frank, E. Piasetzky, V. D. Sandberg, D. A. Krakauer, and R. L. Talaga, *Phys. Rev. D* **47**, 11 (1993).
- [36] D. G. Cerdeño, M. Fairbairn, T. Jubb, P. A. N. Machado, A. C. Vincent, and C. Boehm, *JHEP* **05**, 118 (2016), [Erratum: *JHEP* 09, 048 (2016)], [arXiv:1604.01025 \[hep-ph\]](#).
- [37] Y. Farzan, M. Lindner, W. Rodejohann, and X.-J. Xu, *JHEP* **05**, 066 (2018), [arXiv:1802.05171 \[hep-ph\]](#).
- [38] J. Billard, J. Johnston, and B. J. Kavanagh, *JCAP* **11**, 016 (2018), [arXiv:1805.01798 \[hep-ph\]](#).
- [39] P. Huber, *Phys. Rev. C* **84**, 024617 (2011), [Erratum: *Phys.Rev.C* 85, 029901 (2012)], [arXiv:1106.0687 \[hep-ph\]](#).
- [40] T. A. Mueller *et al.*, *Phys. Rev. C* **83**, 054615 (2011), [arXiv:1101.2663 \[hep-ex\]](#).
- [41] P. Vogel and J. Engel, *Phys. Rev. D* **39**, 3378 (1989).
- [42] M. Lindner, W. Rodejohann, and X.-J. Xu, *JHEP* **03**, 097 (2017), [arXiv:1612.04150 \[hep-ph\]](#).
- [43] M. Bowen and P. Huber, *Phys. Rev. D* **102**, 053008 (2020), [arXiv:2005.10907 \[physics.ins-det\]](#).
- [44] D. Androic *et al.* (Qweak), *Nature* **557**, 207 (2018), [arXiv:1905.08283 \[nucl-ex\]](#).
- [45] C. Patrignani *et al.* (Particle Data Group), *Chin. Phys. C* **40**, 100001 (2016).
- [46] D. Becker *et al.*, *Eur. Phys. J. A* **54**, 208 (2018), [arXiv:1802.04759 \[nucl-ex\]](#).
- [47] P. A. Souder, *Int. J. Mod. Phys. Conf. Ser.* **40**, 1660077 (2016).
- [48] J. Benesch *et al.* (MOLLER), (2014), [arXiv:1411.4088 \[nucl-ex\]](#).
- [49] A. Aguilar-Arevalo *et al.* (CONNIE), *JHEP* **04**, 054 (2020), [arXiv:1910.04951 \[hep-ex\]](#).